ACCOUNTS
of chemical research

Shape-Control and Electrocatalytic Activity-Enhancement of Pt-Based Bimetallic Nanocrystals

NATHAN S. PORTER,[†] HONG WU,[‡] ZEWEI QUAN,[*,†,§] AND JIYE FANG[*,†,‡]

[†]*Department of Chemistry,* [‡]*Materials Science and Engineering Program, State University of New York at Binghamton, Binghamton, New York 13902, United States*

RECEIVED ON JULY 29, 2012

CONSPECTUS

Due to the increasing worldwide energy demand and environmental concerns, the need for alternative energy sources is growing stronger, and platinum catalysts in fuel cells may help make the technologies a reality. However, the pursuit of highly active Pt-based electrocatalysts continues to be a challenge. Scientists developing electrocatalysts continue to focus on characterizing and directing the construction of nanocrystals and advancing their electrochemical applications. Although chemists have worked on Pt-based bimetallic (Pt-M) preparations in the past, more recent research shows that both shape-controlled Pt-M nanocrystals and the assembly of these nanocrystals into supercrystals are promising new directions. A solution-based synthesis approach is an effective technique for preparing crystallographic facet-directed nanocatalysts. This is aided by careful selection of the metal precursor, capping ligand, reducing agent, and solvent. Incorporating a secondary metal M into the Pt lattice and manipulating the crystal facets on the surface cooperatively alter the electrocatalytic behavior of these Pt-M bimetallic nanocrystals. Specifically, chemists have extensively studied the {111}- and {100}-terminated crystal facets because they show unique atomic arrangement on surfaces, exhibit different catalytic performance, and possess specific resistance to toxic adsorbed carbon monoxide (CO_{ads}). For catalysts to have maximum efficiency, they need to have resistance to CO_{ads} and other poisonous carbon-containing intermediates when the catalysts operate under harsh conditions. A necessary design to any synthesis is to clearly understand and utilize the role of each component in order to successfully induce shape-controlled growth. Since chemists began to understand Pt nanocrystal shape-dependent electrocatalytic activity, the main obstacles blocking proton exchange membrane fuel cells are anode poisoning, sluggish kinetics at the cathode, and low activity.

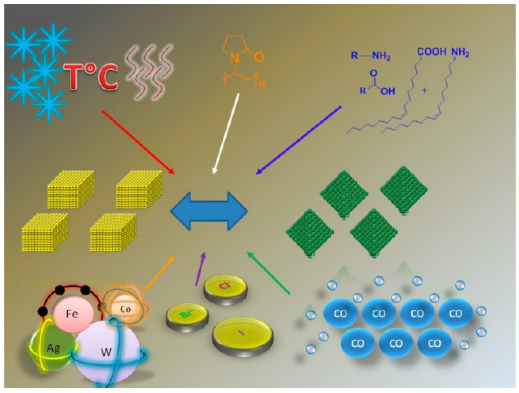

In this Account, we discuss the basic concepts in preparation of Pt-M bimetallic nanocrystals, focusing on several immaculate examples of manipulation at the nanoscale. We briefly introduce the prospects for applying Pt-M nanocrystals as electrocatalysts based on the electronic and geometric standpoints. In addition, we discuss several key parameters in the solution-based synthesis approach commonly used to facilitate Pt-M nanocrystals, such as reaction temperature and time, the combination of organic amines and acids, gaseous adsorbates, anionic species, and solvent. Each example features various nanoscale morphologies, such as spheres, cubes, octahedrons, and tetrahedrons. Additionally, we outline and review the superior electrocatalytic performances of the recently developed high-index Pt-M nanostructures. Next, we give examples of the electrocatalytic capabilities from these shape-defined Pt-M architectures by highlighting significant accomplishments in specific systems. Then, using several typical cases, we summarize electrochemical evaluations on the Pt-based shape-/composition-dependent nanocatalysts toward reactions on both the anode and the cathode. Lastly, we provide an outlook of current challenges and promising directions for shape-controlled Pt-M bimetallic electrocatalysts.

Introduction

It is interesting to seek other energetic resources or different energy conversion pathways to replace the burning of fossil fuels, due to the increasing worldwide energy demand and environmental concerns. A fuel cell is a device that converts the chemical energy of a fuel directly into electricity[1] and is environmentally benign and efficient.[2−6] The use of platinum (Pt) as catalyst in a fuel cell is essential to increase the

Published on the Web 03/05/2013 www.pubs.acs.org/accounts
10.1021/ar3002238

rate of reactions, including hydrogen or small molecule oxidation at the anode and oxygen reduction reaction (ORR) at the cathode. The main obstacles that continue to hinder progress of electrochemical reactions are slow kinetics at the cathode for ORR and the nonreactive oxygenated species (such as CO_{ads}) poisoning at the anode.[7] State-of-the-art carbon-supported Pt nanocrystals (Pt/C NCs) are still the effective electrocatalysts in fuel cell technology. Due to the scarcity of Pt and the fact that there has been little progress in complete replacement of Pt in fuel cells, however, dramatic decreases in the amount of Pt are required and an alternative solution is needed. Therefore, Pt-based bimetallic (hereafter, denoted as "Pt-binary") NCs, that is, Pt alloys with less expensive secondary transition metals, M, have been proposed as substitutes of the fuel cell catalysts.[8−18] Another reason of developing Pt-binary catalysts is due to their superior catalytic performance compared to Pt NCs,[12] because the incorporation of M in the NC alters the surface electronic structure of Pt and modifies its *d*-band center position. As a result, the interaction between the Pt surface atoms and poisonous intermediate is weakened and the resistance to poisonous substances is therefore enhanced.[19,20]

The catalytic performance of Pt-binary catalysts is dependent on their crystal facet.[20] Well-defined shapes of Pt-based nanocatalysts mimic the catalytic property of the bulk metal but show superior catalytic activity due to an increased number of active sites.[21] It is therefore a promising route to "transfer" the active catalytic surface from a single crystal to more practical nanophase by establishing a shape-control synthesis strategy. Early research led by El-Sayed et al. shed light on promising directions in shape-controlled synthesis of NCs, although they focused on the catalytic properties of single Pt only, including {111}-bounded nanotetrahedra, {100}-terminated nanocubes (NCbs), and "near spherical" NCs containing a mixture of {111} and {100} facets.[22,23] Following this work, it was further confirmed that a catalytic performance is dependent on the surface atom arrangement, that is, morphologic characteristics.[24]

In this Account, the mainstay is the shape-control of Pt-M bimetallic NCs. After a short introduction to bimetallic NCs, we focus on Pt-M bimetallic NC synthesis with a discussion on influences from several important chemisorbed species. A special case concerning high-index Pt-M bimetallic NC synthesis is then given. Eventually, a general outline on shape- and composition-dependent electrochemical properties, current challenges, and future prospects in this field are provided.

Pt and Pt−M Bimetallic Nanocatalyst Foresight

In a Pt-M NC, it is known that the atomic packing arrangement of distinct Pt and corresponding M atoms could be ordered with a stoichiometric local composition[25] or distributed randomly for one another. As for the crystal facets, it is believed that the surface energy of a *face-centered-cubic* (*fcc*) Pt NC in different crystal planes increases in an order of $\gamma(111) < \gamma(100) < \gamma(110) < \gamma(hkl)$.[26] Accordingly, NC growth may occur by adatom incorporation perpendicular to high-energy crystal planes that are therefore expected to rapidly vanish due to their low stability. This leads to an observation of only low-index facets, although talented synthesis has yielded high-index NCs recently (*vide infra*).[27,28] Theoretical calculations suggested that the size of a Pt cluster affects its final NC morphology.[29−31] A practical solution synthesis normally consists of a nucleation stage where the released metal atoms combine into clusters in various sizes[32] and a NC growth where such clusters find a configuration and form "cores" with a specific shape in order to minimize their overall interfacial free energy.[33] The final shape of a Pt or Pt−M NC is a competition among surface energies of different facets.

Preparation of Bimetallic Nanocrystals: A General Case

1. Effects of Foreign Metal, Temperature, Capping Agent, Reaction Time, and Solvent. To control the shape of NCs, a foreign metal protocol was used in a solution-based synthesis of Pt. For example, when iron (Fe) ions such as Fe^{2+} and Fe^{3+} present in solution, the Pt ions do not reach a critical cluster concentration as rapidly, allowing an isotropic growth.[34] In addition, silver (Ag) ions were found to preferentially stabilize specific facets of the Pt NC. By tuning the concentration of Ag^{+}, a formation of NCs in various morphologies was reported.[35] In a $W(CO)_6$-based synthesis,[36] the control of NC shape relies on a decomposition rate of the metal−carbonyl and competitive nucleation of Pt and M. This has been demonstrated in synthesis of Pt, Pt_3Co, Pt_3Fe, and Pt_3Ni NCbs (Figure 1).[19,37−39] In this example, NCbs were readily formed in a mixture of oleylamine (OAm) and oleic acid (OA) in a fixed ratio. The roles of OAm, OA, and their synergistic combination effect are significant. It is known that OAm possibly slows down successive NC growth and prevents NC agglomeration. A small amount of OA improves the OAm's effectiveness, although itself may hinder the generation of NCbs by causing a precipitation or producing small irregular NCs.[17,36] Synthesis of Pt_3Ni NCbs required a titration of the Ni-precursor due to the readiness of Ni in alloying with Pt, ultimately slowing down the

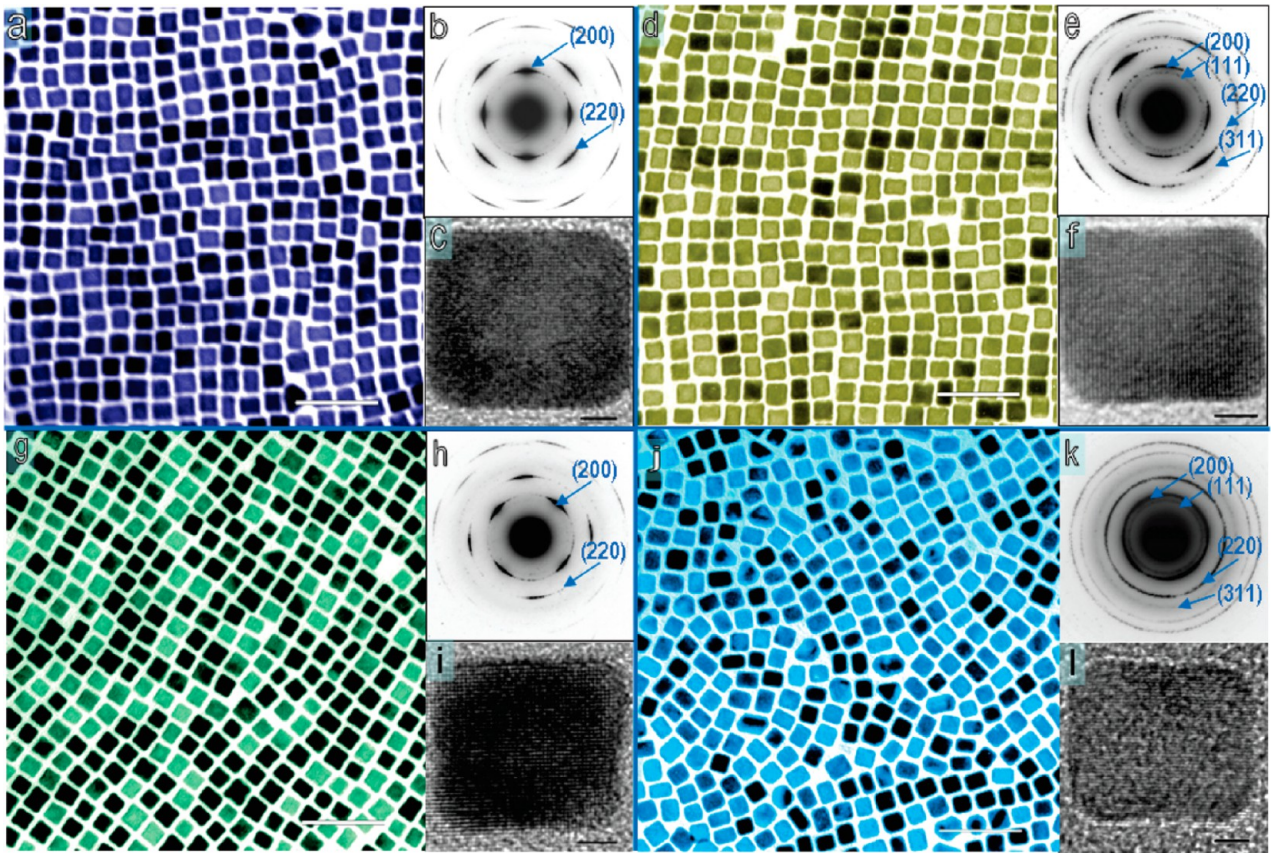

FIGURE 1. TEM images and diffraction patterns: (a–c) Pt nanocubes; (d–f) Pt_3Co nanocubes; (g–i) Pt_3Fe nanocubes; and (j–l) Pt_3Ni nanocubes. Data bars in (a, d, g, and j) and (c, f, i, and l) represent 50 and 2 nm, respectively. Adapted with permission from ref 36. Copyright 2009 American Chemical Society.

reaction kinetics and generating {100}-terminated low-energy facets.[37] It was hypothesized that OAm/OA and the yielded W^0 act as reducing agent at high temperature, and are essential in shape-control of the binary NCs. Not only were NCbs prepared using this approach, but also Pt_3Ni nano-octahedra can be fabricated through the same one-pot synthesis in which a slow addition of the Ni precursor must be avoided (Figure 2). The W^0 is reactive and causes a rapid reduction of Pt^{2+}, preserving Pt for a specific growth mode along the NC surface.[37] In another instance, $Cr(CO)_6$ was used to prepare Pt NCs.[40] Due to the susceptibility of Cr being oxidized, it was removed from the Pt lattice and remained as an ionic species in solution.[40] Such a role of foreign metal Cr can be further confirmed in the following preparation: when $Cr(CO)_6$ was used to prepare Pt nanowires, less than 1% Cr could be detected in the products,[41] indicating its propensity of reducing Pt ions rather than "alloying" with Pt.

The next example is a synthesis of PtFe NCs in which the temperatures for $Fe(CO)_5$ decomposition and that for Pt nucleation match very well (Figure 3a–d).[42] To ensure an equal concentration of Fe- and Pt-atom generated prior to the conucleation stage, 1,2-hexadecanediol was used to enhance the reduction of Pt^{2+} from its precursor in addition to OAm/OA. Cubic PtFe NCs were further prepared using a similar system, but the addition sequence of OAm/OA and Fe/Pt ratio in the precursors were altered.[43] A hot injection of $Mn_2(CO)_{10}$ stock solution into a mixture containing Pt, OAm, and OA in benzyl ether at an elevated temperature could also generate a formation Pt–Mn NCbs (Figure 3e and f). However, a room temperature injection only resulted in spherical Pt–Mn NCs that are terminated with a mixture of {111} and {100} facets.[44] It was also reported that Pt_3Sn spherical NCs could be generated via a simultaneous hot-injection of both precursors to a solution containing OAm/OA (ca. 1.5:1 in mol ratio).[45] As an additional example with respect to the growth time, Pt_3Co truncated nano-octahedra were prepared using $Co_2(CO)_8$, in the presence of hexadecanediol and OAm/OA (ca. 8:1 in mol ratio). By simply increasing the reaction time from 30 to 90 min at 200 °C, truncated nano-octahedra could be converted to NCbs.[46] As for the solvent effect, Pt–Zn spherical NCs were prepared in OAm/OA (ca. 6:1 in mol ratio) at 350 °C. NCbs could be

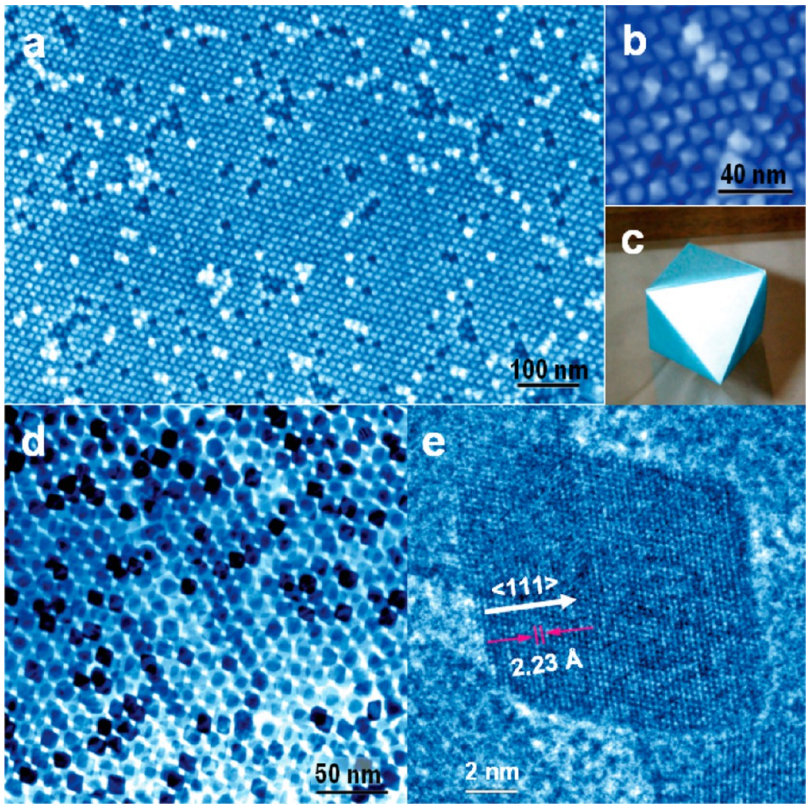

FIGURE 2. EM images of Pt_3Ni nano-octahedra. (a) Field-emission SEM image; (b) HRSEM image; (c) 3D image of an octahedron; (d) TEM image; (e) HRTEM image of single nanocrystal. Adapted with permission from ref 37. Copyright 2010 American Chemical Society.

further harvested when benzyl ether was introduced in the system and the volume of OAm/OA was reduced by half (Figure 3g–j). The high temperature, appropriate ratio between OAm/OA and noncoordination solvent benzyl ether was quintessential in generating the NCbs as well as incorporating Zn atoms into the Pt lattice.[47] Recently, Pt_3Pb spherical NCs were prepared through hot injection of a strong reducing agent in the presence of OAm/OA (ca. 6:1 in volume ratio) at 180 °C. Alternately, the use of R-NH_2 and R-COOH led to nanorods.[48] A noble gas stream was used in above syntheses.

2. Effect of CO Reduction. Another substantial study in terms of Pt-based shape-controlled NCs was based on the work of carbon monoxide (CO) reducing/binding effects. It was reported that Pt NCbs could be facilitated in the presence of CO with a fixed ratio of OAm/OA and an optimized period of growth time.[49,50] It was suggested that CO functions as a reducing agent rather than a capping ligand.[49] A continuation of this work led to a gas-template synthesis of shape-controlled Pt-M (M = Ni, Co, Fe, Pd) NCs when additional solvent/capping ligands were also involved in some cases.[51] To prepare Pt–Ni NCbs, for instance, reaction mixtures were preplaced in an oil bath at 130 °C under argon atmosphere, and then transferred to a second oil bath at 210 °C under CO atmosphere for 30 min. OAm and OA (ca. 9:1 in volume ratio) were employed to help facilitate the {100}-enclosed Pt–Ni NCbs. Conversely, in order to prepare Pt–Ni (or Pt–Co) nano-octahedra, an equal volume of diphenyl ether was used in place of OA while all other reaction conditions remained the same.[51] This protocol was also applied to syntheses of Pt–Au, Pt–Ni, and Pt–Pd nanoicosahedra (Figure 4).[52] It was believed that CO could assist in developing Pt-based NCs in certain shape.[49,51]

3. Effect of Anionic Species. Halogen ions can also stabilize {100} crystal planes of metal NCs,[53–55] such as ~55 nm Ag NCbs in an aqueous system. The mechanism of formation entails the chemisorption of Br^- ions on the {100} crystal surface and prevents further addition of metal ions thereafter.[54] Sub-25 nm Pd and Pt NCbs and nanorods were shown to have stabilized crystal planes in the presence of these halogen ions and poly(vinyl pyrrolidone) (PVP). Specifically, Br^- ions show the most pronounced effects on {100} stabilization. In a polyol synthesis, these ions could act as {100}-stabilizers as well as oxidative etchants.[53] Such a function of halogen ions was extended beyond single metal systems, resulting in pristine bimetallic NCbs such as 10 nm

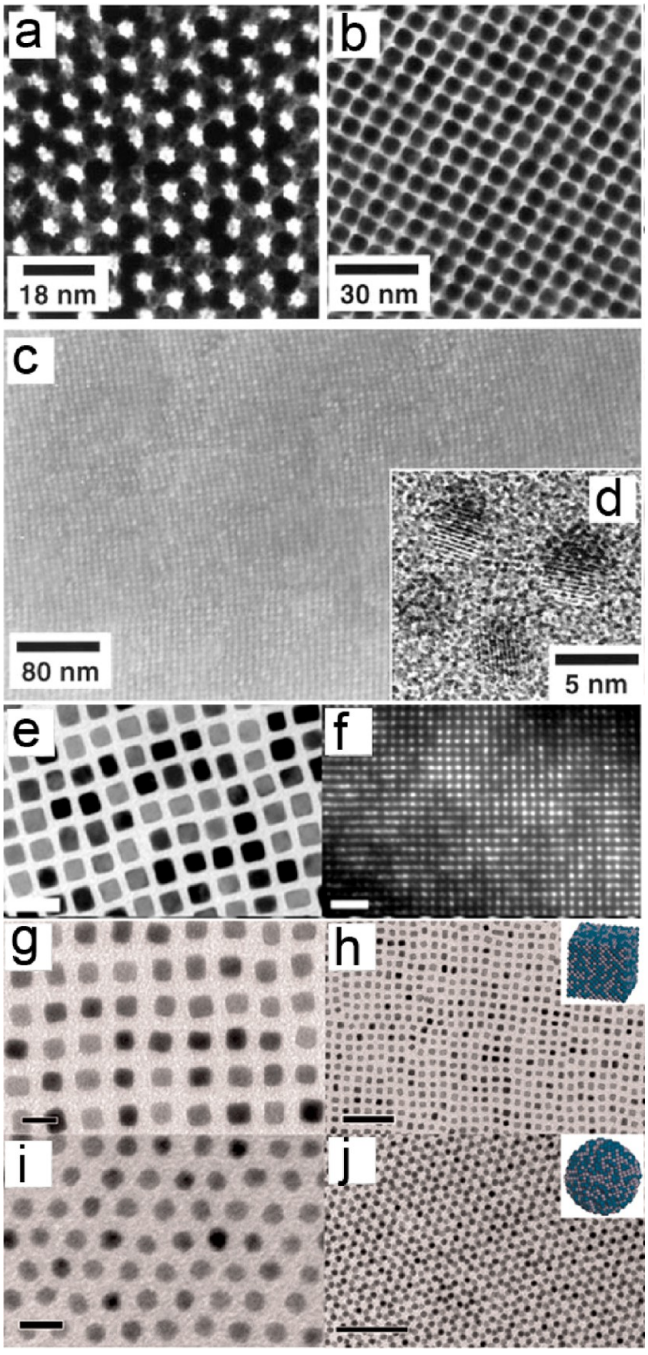

FIGURE 3. (a) TEM micrograph of a 3D assembly of 6-nm as-synthesized $Fe_{50}Pt_{50}$ particles; (b) TEM micrograph of a 3D assembly of 6 nm $Fe_{50}Pt_{50}$ sample after replacing ligand replacement; (c) HRSEM image of annealed $Fe_{52}Pt_{48}$ nanocrystal assembly; (d) HRTEM image of 4 nm $Fe_{52}Pt_{48}$ annealed nanocrystals. Adapted with permission from ref 42. Copyright 2000 American Association for the Advancement of Science. TEM images of Pt−Mn nanocubes (e) and a large area of self-assembly (f). Adapted with permission from ref 44. Copyright 2010 American Chemical Society. (g,h) TEM images of cubic Pt−Zn NCs and (i,j) TEM images of spherical Pt−Zn nanocrystals. Insets in (b) and (d) are graphic models of Pt−Zn cubic nanocrystals and spherical nanocrystals. The gray and blue balls represent Zn and Pt atoms, respectively. Scale bars: (g,i) 10 nm and (h,j) 50 nm. Adapted with permission from ref 47. Copyright 2012 American Chemical Society.

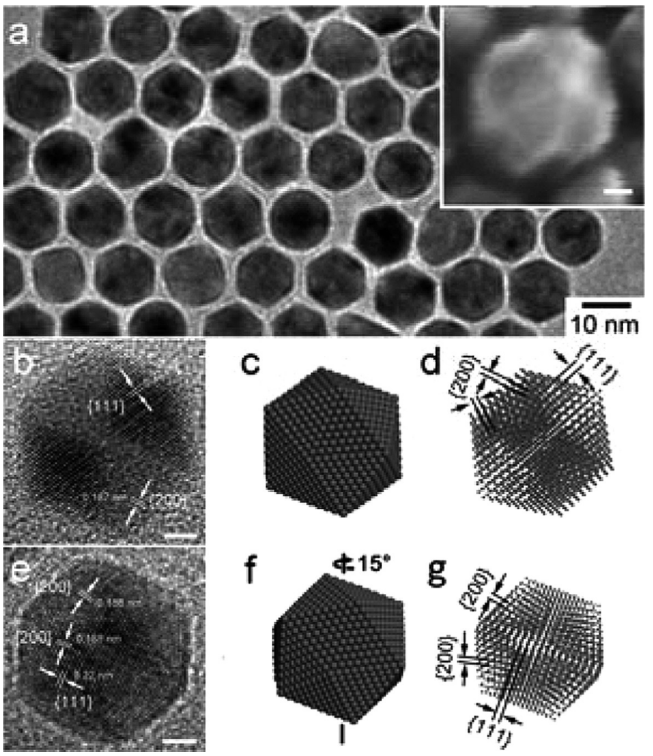

FIGURE 4. EM images of Pt_3Ni NCs. (a) TEM and SEM (inset); and (b−g) HRTEM micrographs and 3D models of Pt_3Ni icosahedral nanocrystals at two different orientations, respectively. The scale bars correspond to 2 nm. Adapted with permission from ref 52. Copyright 2012 American Chemical Society.

Pt−Pd NCbs (Figure 5b).[55] The trick to success in this process is a fine-tuning of the Br^-/I^- ratio (Figure 5b and d).[55] Moreover, as shown in Figure 5a, c, and e,[55] it is possible to facilitate {111}-bounded Pt−Pd nanotetrahedra in a similar system when formaldehyde and oxalate ions were used as the reducing agent and capping ligand, respectively. Finally, this strategy was extended to an organic solution-based system, where alkyl ammonium salts were implemented to yield halogen ions that served as a crystal surface stabilizing agent. As an example, PtCu NCbs were prepared in an organic system containing dodecanethiol and OAm, where tetraoctylammonium bromide was utilized as a stabilizing agent.[17]

High-Index Nanocrystals: A Special Case

It was suggested that high-index-surface terminated NCs could enhance their catalytic performance.[56] Sun et al. demonstrated their preparation of high-index Pt tetrahexahedral (THH) NCs using an electrochemical square-wave potential (ESWP) method.[28] One of the driving forces of the Pt THH formation is the surface $Pt-O_2$ exchange interaction. Using deep eutectic solvents as a medium, seeds are not

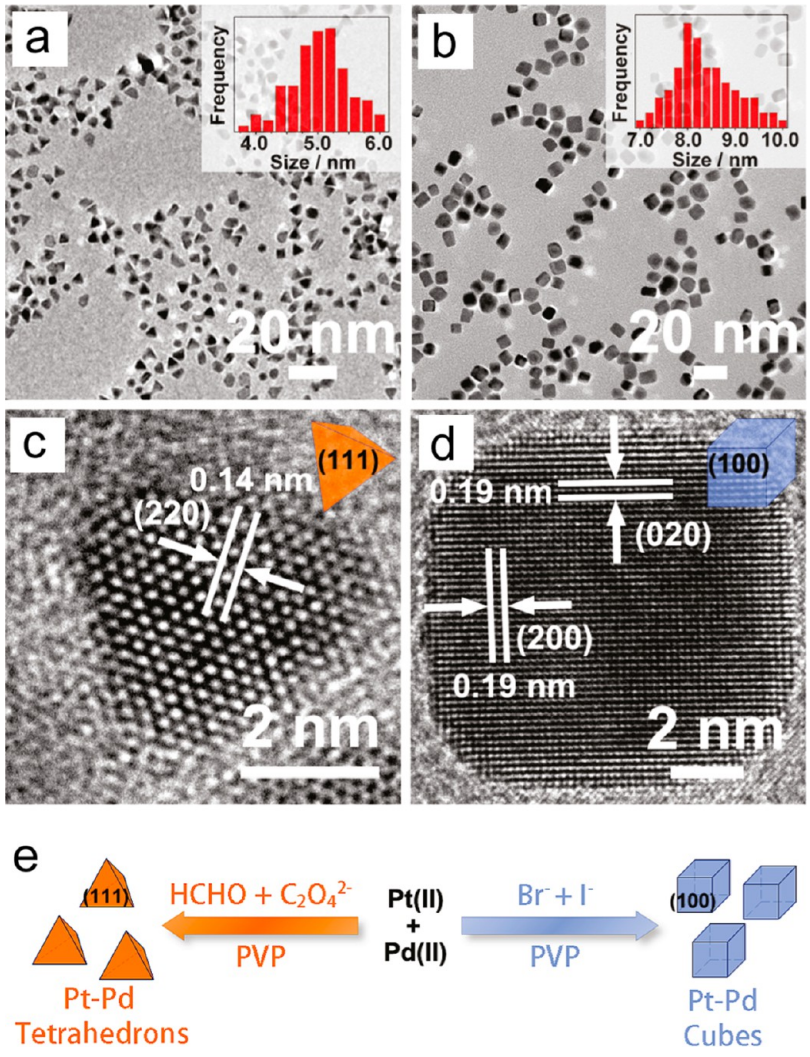

FIGURE 5. TEM images: (a) the Pt−Pd nanotetrahedrons; (b) nanocubes; (c) HRTEM image of a single Pt−Pd nanotetrahedron; (d) HRTEM image of a single nanocube; (e) Schematic illustration of shape-selective synthesis of Pt−Pd nanotehedrons and nanocubes. Adapted with permission from ref 55. Copyright 2011 American Chemical Society.

necessary and the morphology of {910}-faceted Pt THH NCs can be controlled by adjusting the upper and lower cycling potentials.[57] Pt high-index facets, such as {510}, {720}, and {830}, have been determined on Pt concave NCbs prepared through a reduction reaction in an aqueous solution (Figure 6a−c),[58] and these high-index Pt NCs exhibit comparatively enhanced electrocatalytic activity (Figure 6d).[58] Since Pt-binary NCs were poised as superior electrocatalysts, their concave NCbs were assumed to possess promising electrochemical performance and have been proved. For instance, high-index Pt−Pd concave NCbs with different contents of Pt were prepared through a site-selective galvanic replacement reaction between $PtCl_6^{2-}$ ions and Pd NCbs (Figure 6e).[59] Their ORR performance with 3.4 wt % Pt exhibited the largest specific electrochemical surface area and was four times more active than the commercial Pt/C catalyst on the basis of equivalent Pt mass (Figure 6f). Another example is the preparation of high-index Pt−Cu and Pt−Pd−Cu concave NCbs.[60] In this hydrothermal-assisted process, the abundance of Br^- species in solution could alter the reaction kinetics by inhibiting the growth on {100} crystal planes. As a result, concentration of $[PtBr_4]^{2-}$ might be higher near the (100) facets, and Cu atoms could be easily oxidized and then dissolved into the solution, forming a concave structure.[60] As shown in Figure 6g and h, both specific and mass activities for methanol oxidation reaction (MOR) on these concave structures are superior to those of low-indexed NCbs. Surface segregation of Pt and M may also be achieved by dealloying methods, such as acid dissolution of a less noble metal or potential cycling. In either case, enhanced catalytic activity was determined compared to that of the state-of-the-art Pt/C. MOR evaluations on PtCo

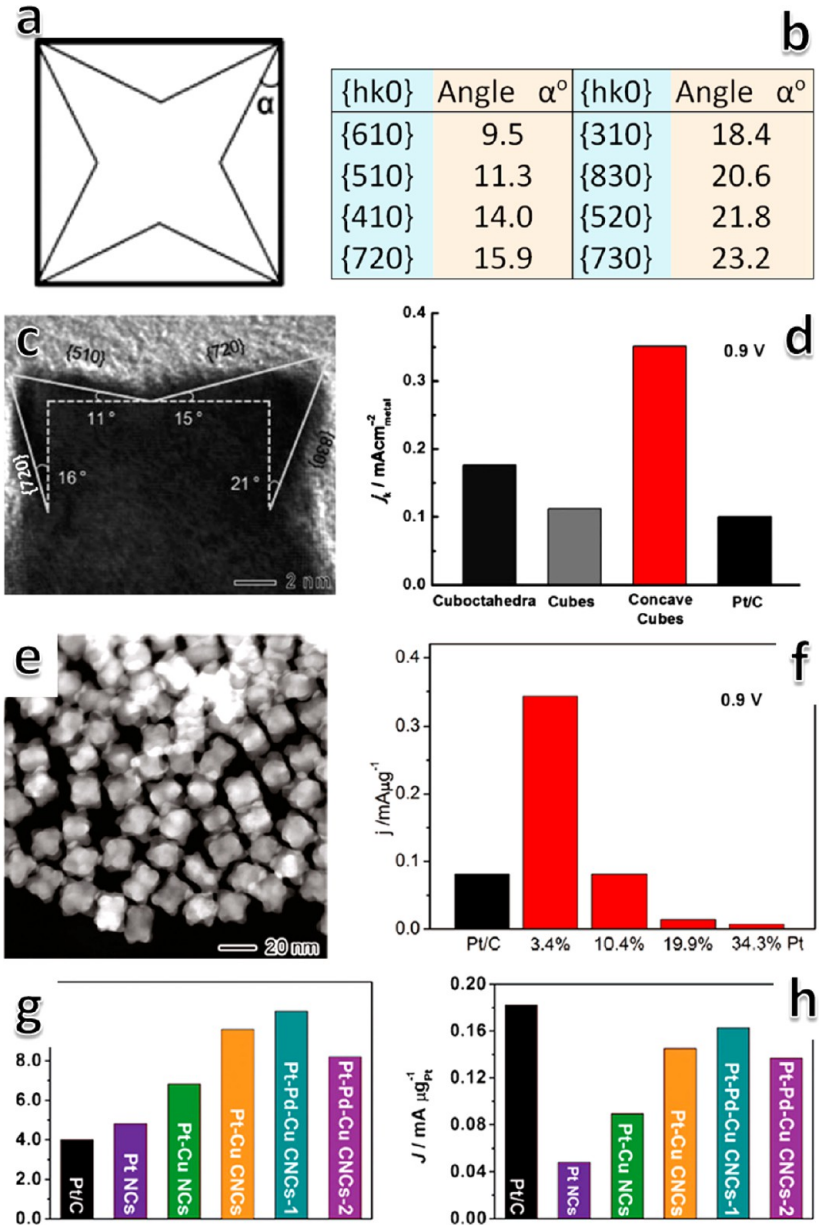

FIGURE 6. Concave nanocubes. (a,b) Theoretical relationship between interfacial angles and high-index factes; (c) HRTEM image of a Pt concave nanocube; (d) specific activities of Pt NCs at 0.9 V vs RHE. The metal loading on the glassy carbon electrode was 15.3 mg cm^{-2}. Adapted with permission from ref 58. Copyright 2011 Wiley. (e) High-angle annular dark-field scanning TEM image of Pt–Pd concave nanocubes; (f) mass activities of Pt–Pd NCs (normalized by the weight of Pt) at 0.9 V vs RHE. For comparison, Pt/C was included. Adapted with permission from ref 59. Copyright 2011 American Chemical Society. (g) Specific activities and (h) mass activities of Pt, Pt–Cu, and Pt–Pd–Cu low-indexed nanocubes and high-index concave nanocubes for methanol oxidation reaction. For comparison, Pt/C was included. Adapted with permission from ref 60. Copyright 2012 Wiley.

nanowires[61] and ORR evaluation on Pt–Ni spherical NCs[62] prepared through an integration of the dealloying and other technique are impressive examples.

Evaluation on Electrochemical Property of Bimetallic Nanocrystals

As mentioned, incorporating M into Pt lattices may improve their catalytic performance through bifunctional and electronic structure alteration mechanisms. As an example of MOR, M is mainly responsible for the water dehydration to form M–OH transition state while Pt catalyzes most methanol to form Pt–CO_{ads} according to the bifunctional mechanism.[63] Electrochemical evaluation on Pt–Pd bimetallic NCs for MOR supports this argument,[64] indicating that the activity and stability toward MOR are highly dependent on the composition of electrocatalysts.[64] The peak potentials and peak current densities of MOR show a "maximum activity plateau" for Pt–Pd catalyst with 40–60% Pt, as presented in Figure 7a and b.

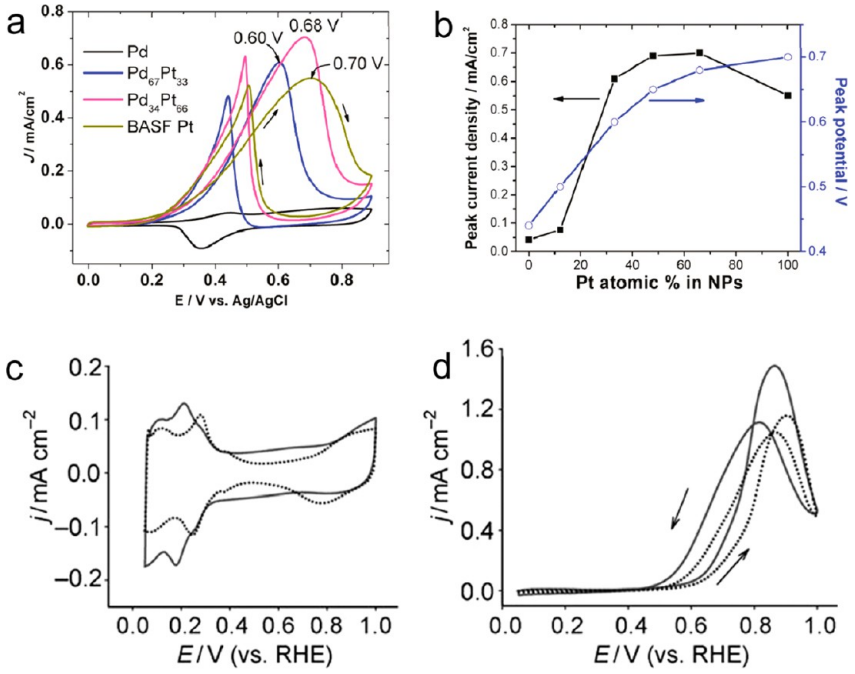

FIGURE 7. (a) *J*−*V* curves reflecting methanol oxidation catalysis of nanoparticle catalysts in 0.1 M $HClO_4$ + 0.1 M methanol; (b) methanol oxidation peak current density and peak potential vs the Pt atomic % in Pt−Pd nanoparticles. Adapted with permission from ref 64. Copyright 2011 American Chemical Society. (c) Cyclic voltammorgrams of Pt_3Co (solid line) and Pt nanocubes (dotted line) in 0.1 M $HClO_4$ (scan rate: 0.1 V s^{-1}); (d) cyclic voltammorgrams of methanol oxidation on Pt_3Co (solid line) and Pt nanocubes (dotted line) in 0.1 M $HClO_4$ +1 M MeOH (scan rate: 0.02 V s^{-1}). Adapted with permission from ref 39. Copyright 2010 Wiley.

Due to the presence of Pd, the water dehydrogenation on Pt occurs at a lower potential, thereby providing an effective oxidation reaction overall.[64] In Pt_3Sn, adsorption between Pt and CO is weakened due to the presence of Sn, and it was believed that such bimetallic NCs are more active toward MOR and CO oxidation.[45] According to the electronic structure change theory, on the other hand, the *d*-band center of Pt largely shifts, partially due to the presence of M. This results in a lower adsorption energy of poisonous carbon intermediates.[65] It has been demonstrated that {100}-terminated Pt_3Co NCbs possess a higher activity of MOR compared to Pt NCbs.[39] The former exhibits a superior current density at a lower onset potential with respect to the Pt NCbs (Figure 7c and d).

Pt−Cu NCbs, as an example, show improved methanol and formic acid oxidation activities compared to those with other shapes, indicating that the oxidation activity of small organic species is strongly dependent on the surface structure of Pt-binary catalysts.[20] As shown in Figure 8a and b, the MOR activity follows an order of Pt−Cu NCbs > Pt−Cu nanospheres > Pt nanospheres in $HClO_4$, suggesting that the {100}-bounded Pt−Cu NCbs offer a greater activity enhancement than those with mixed facets.[17] At the cathode, ORR activities of Pt_3Ni NCbs and nano-octahedra were also comparatively explored,[37] showing that the mass/specific ORR activities of the nano-octahedra are ~2.8/~5.0 times of that of the Pt_3Ni NCbs and ~3.6/~6.5 times of Pt NCbs at 0.9 V/RHE (Figure 8c and d).[37] The specific and mass activities of such Pt_3Ni nano-octahedra loaded on active carbon are ~7 and ~4 times higher than those of state-of-the-art Pt/C catalysts, respectively.[20] Pt_3Co truncated nano-octahedra also exhibit ORR improvements with a superior activity compared to Pt_3Co NCbs and to Pt/C.[46] These studies confirmed the strong shape-dependent ORR activity of Pt-binary NCs with respect to exposed planes in $HClO_4$ electrolyte, and the results are consistent with the conclusion from extended surface studies (Figure 8e and f).[15,66]

It should be pointed out that the catalytic evaluation is also dependent on the reaction medium. It was reported that an activity sequence on Pt(hkl) for the ORR is Pt(111) < Pt(100) < Pt(110) in H_2SO_4,[67] whereas the order in 0.1 M KOH is Pt(100) < Pt(110) < Pt(111),[68] and in nonadsorbing $HClO_4$ electrolyte it is Pt(100) < Pt(110) ≪ Pt(111).[69] In H_2SO_4, Pt {100} facets are more active toward ORR than in $HClO_4$ due to the bisulfate anion adsorption.[70] Pt{111} surfaces reveal a higher ORR activity compared to other low-index surfaces in KOH and especially in $HClO_4$ due to selective adsorption of OH_{ads} on Pt{111} surfaces where the threat of irreversible surface damage during O_2 adsorption is also

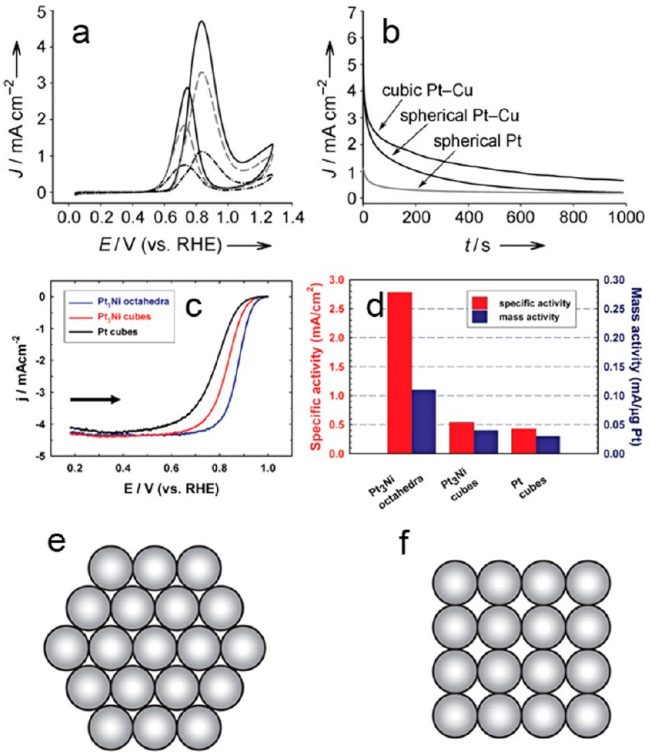

FIGURE 8. (a) Cyclic voltammorgrams of methanol oxidation on Pt–Cu NCbs (—), Pt–Cu nanospheres (– – –), and Pt nanospheres (–·–·–) in 0.1 M $HClO_4$ + 1 M MeOH (scan rate: 0.02 V s^{-1}); (b) chronoamperometric results of MeOH oxidation at 0.8 V on Pt–Cu nanicubes, Pt–Cu nanospheres, and Pt nanospheres in 0.1 M $HClO_4$ + 1 M MeOH. Adapted with permission from ref 17. Copyright 2009 Wiley. (c) Polarization curves for ORR on Pt3Ni nano-octahedra, Pt_3Ni nanocubes, and Pt nanocubes supported on a rotating GC disk electrode; (d) comparison of the ORR activities on the three types of catalysts. Specific and mass activities were measured at 0.9 V vs RHE at 295 K. Adapted with permission from ref 37. Copyright 2010 American Chemical Society. (e) Surface structure on a nano-octahedron of Pt_3Ni; (f) surface structure of a nanocube of Pt, Pt–Cu, or Pt_3Ni.

prevented. Such a medium-dependent change was also observed in Pt-binary systems. Pt–Mn NCbs exhibit a higher ORR specific activity in H_2SO_4 than in $HClO_4$, although they already present a higher activity for MOR than state-of-the-art Pt/C and spherical Pt–Mn NCs do.[44]

In contrast with low-index facets({100}, {110}, and {111}), high-index surfaces {*hkl*} are the key to boost catalytic performance owing to the large number of exposed atomic steps, edges, and kinks. Pt concave NCbs bound by {720} facets do demonstrate greater ORR specific activity than Pt NCbs and nanocuboctahedra, which expose low-index facets only.[58] MOR activity of Pt–Ni bimetallic "nanobundles", depicted as a branched structure containing stepped surfaces, is ~3.6 times of that of Pt NCs due to its high density of atomic surface steps existing along the "nanobundles".[71] Pt–Pd bimetallic nanodendrites were 2.5 times more active on the basis of equivalent Pt mass for the ORR than state-of-the-art Pt/C catalyst,[72] and Pt-on-Pd bimetallic heteronanostructures demonstrated a long-term stability.[73] The high-index facets {*hk*0} class of Pt–Cu and Pt–Pd–Cu concave NCbs also presented superior MOR activities.[60] Their catalytic discussion has been given above (Figure 6f, g).

Current Challenges and Highlights

In comparison with single metallic NCs, preparation of Pt-binary NCs is much more complicated and challenging. It was demonstrated that shape-controlled Pt and Pt-M NCs could offer great advantages in improving the performance of fuel cell nanocatalysts. However, activity enhancement by a factor of 5–10 remains elusive for ORR, in comparison with the bulk extended surface catalysts. To minimize the gap and improve stability, further improvement on Pt-based NCs is expected. One of the proposed strategies is to mimic the extended Pt-skin surface and to create Pt-binary NCs with more active atomic sites for promotion of electrocatalytic performance. Selective and high-index crystallographic facet synthesis of Pt-binary NCs might be an interesting direction to facilitate electrocatalysts used in near future fuel cell technology set-ups.

This work was partially supported by General Motors LLC, DOE, and SUNY-Binghamton. N.S.P. thanks Clifford E. Mayers summer research grant.

BIOGRAPHICAL INFORMATION

Nathan S. Porter was born in Cortland, NY in 1987. He received his B.Sc. degree in Chemistry from Clarkson University in 2009. He is pursuing his Ph.D in Chemistry Department at SUNY-Binghamton with Dr. Jiye Fang. His current research interests include synthesis and evaluation of shape-controlled Pt-based nanocrystals.

Hong Wu was born in Shanghai, China in 1986. She received her B.Eng. degree in Materials Science and Engineering (2008) from Tongji University, China. She is a graduate student in Materials Science and Engineering program at SUNY-Binghamton with Dr. Jiye Fang. Her current research work focuses on the electrochemical study of Pt-Based nanocatalyst performance.

Zewei Quan was born in Luoyang, China in 1982. After obtaining his B.Sc. degree in Chemistry from Wuhan University in 2004, he received a Ph.D. degree from Chinese Academy of Sciences (with Prof. Jun Lin) in 2009. He was a postdoctoral fellow and then a research scientist in Department of Chemistry at SUNY-Binghamton with Dr. Jiye Fang. His current research interests include synthesis and self-assembly of nanostructured materials.

Jiye Fang is currently an Associate Professor of Chemistry and Director of Materials Science Program/track at SUNY-Binghamton.

After he graduated from Lanzhou University, he received his M.Sc. in Chemistry and Ph.D. in Materials Science from National University of Singapore in 1994 and 1998, respectively. His research direction is shape-control synthesis of functional low-dimensional materials.

FOOTNOTES

*To whom correspondence should be addressed. E-mail: jfang@binghamton.edu (J.F.); zquan@lanl.gov (Z.Q.).

The authors declare no competing financial interest.

[§]Z.Q.: EES-14 and MPA-MSID, Los Alamos National Laboratory, Los Alamos, New Mexico 87545, United States.

REFERENCES

1 Khurmi, R. S.; Sedha, R. S. *Materials Science*, 5th ed.; S. Chand & Company Ltd.: New Delhi, DEL, India, 2010.

2 Dresselhaus, M. S.; Thomas, I. L. Alternative Energy Technologies. *Nature* **2001**, *414*, 332–337.

3 Gasteiger, H. A.; Kocha, S. S.; Sompalli, B.; Wagner, F. T. Activity Benchmarks and Requirements for Pt, Pt-Alloy, and Non-Pt Oxygen Reduction Catalysts for PEMFCs. *Appl. Catal., B* **2005**, *56*, 9–35.

4 Steele, B. C. H.; Heinzel, A. Materials for fuel-cell technologies. *Nature* **2001**, *414*, 345–352.

5 Winter, M.; Brodd, R. J. What Are Batteries, Fuel Cells, and Supercapacitors? *Chem. Rev.* **2004**, *104*, 4245–4270.

6 Vielstich, W.; Lamm, A.; Gasteiger, H. A. *Handbook of Fuel Cells: Fundamentals, Technology, Applications*; Wiley: New York, 2003.

7 Wagner, F. T.; Lakshmanan, B.; Mathias, M. F. Electrochemistry and the Future of the Automobile. *J. Phys. Chem. Lett.* **2010**, *1*, 2204–2219.

8 Koh, S.; Leisch, J.; Toney, M. F.; Strasser, P. Structure-Activity-Stability Relationships of Pt−Co Alloy Electrocatalysts in Gas-Diffusion Electrode Layers. *J. Phys. Chem. C* **2007**, *111*, 3744–3752.

9 Koh, S.; Strasser, P. Electrocatalysis on Bimetallic Surfaces: Modifying Catalytic Reactivity for Oxygen Reduction by Voltammetric Surface Dealloying. *J. Am. Chem. Soc.* **2007**, *129*, 12624–12625.

10 Mukerjee, S.; Srinivasan, S. Enhanced Electrocatalysis of Oxygen Reduction on Platinum Alloys in Proton Exchange Membrane Fuel Cells. *J. Electroanal. Chem.* **1993**, *357*, 201–224.

11 Paulus, U. A.; Wokaun, A.; Scherer, G. G.; Schmidt, T. J.; Stamenkovic, V.; Radmilovic, V.; Markovic, N. M.; Ross, P. N. Oxygen Reduction on Carbon-Supported Pt−Ni and Pt−Co Alloy Catalysts. *J. Phys. Chem. B* **2002**, *106*, 4181–4191.

12 Serov, A.; Kwak, C. Review of Non-Platinum Anode Catalysts for DMFC and PEMFC Application. *Appl. Catal., B* **2009**, *90*, 313–320.

13 Stamenkovic, V.; Schmidt, T. J.; Ross, P. N.; Markovic, N. M. Surface Composition Effects in Electrocatalysis: Kinetics of Oxygen Reduction on Well-Defined Pt_3Ni and Pt_3Co Alloy Surfaces. *J. Phys. Chem. B* **2002**, *106*, 11970–11979.

14 Stamenković, V.; Schmidt, T. J.; Ross, P. N.; Marković, N. M. Surface Segregation Effects in Electrocatalysis: Kinetics of Oxygen Reduction Reaction on Polycrystalline Pt_3Ni Alloy Surfaces. *J. Electroanal. Chem.* **2003**, *554−555*, 191–199.

15 Stamenkovic, V. R.; Mun, B. S.; Arenz, M.; Mayrhofer, K. J. J.; Lucas, C. A.; Wang, G.; Ross, P. N.; Markovic, N. M. Trends in Electrocatalysis on Extended and Nanoscale Pt-Bimetallic Alloy Surfaces. *Nat. Mater.* **2007**, *6*, 241–247.

16 Watanabe, M.; Tsurumi, K.; Mizukami, T.; Nakamura, T.; Stonehart, P. Activity and Stability of Ordered and Disordered Co-Pt Alloys for Phosphoric Acid Fuel Cells. *J. Electrochem. Soc.* **1994**, *141*, 2659–2668.

17 Xu, D.; Liu, Z.; Yang, H.; Liu, Q.; Zhang, J.; Fang, J.; Zou, S.; Sun, K. Solution-Based Evolution and Enhanced Methanol Oxidation Activity of Monodisperse Platinum−Copper Nanocubes. *Angew. Chem., Int. Ed.* **2009**, *48*, 4217–4221.

18 Mukerjee, S.; Srinivasan, S.; Soriaga, M. P.; McBreen, J. Role of Structural and Electronic Properties of Pt and Pt Alloys on Electrocatalysis of Oxygen Reduction. *J. Electrochem. Soc.* **1995**, *142*, 1409–1422.

19 Lim, S. I.; Ojea-Jiménez, I.; Varon, M.; Casals, E.; Arbiol, J.; Puntes, V. Synthesis of Platinum Cubes, Polypods, Cuboctahedrons, and Raspberries Assisted by Cobalt Nanocrystals. *Nano Lett.* **2010**, *10*, 964–973.

20 Stamenkovic, V. R.; Fowler, B.; Mun, B. S.; Wang, G.; Ross, P. N.; Lucas, C. A.; Marković, N. M. Improved Oxygen Reduction Activity on $Pt_3Ni(111)$ via Increased Surface Site Availability. *Science* **2007**, *315*, 493–497.

21 Chen, J.; Lim, B.; Lee, E. P.; Xia, Y. Shape-Controlled Synthesis of Platinum Nanocrystals for Catalytic and Electrocatalytic Applications. *Nano Today* **2009**, *4*, 81–95.

22 Ahmadi, T. S.; Wang, Z. L.; Green, T. C.; Henglein, A.; El-Sayed, M. A. Shape-Controlled Synthesis of Colloidal Platinum Nanoparticles. *Science* **1996**, *272*, 1924–1925.

23 Narayanan, R.; El-Sayed, M. A. Catalysis with Transition Metal Nanoparticles in Colloidal Solution: Nanoparticle Shape Dependence and Stability. *J. Phys. Chem. B* **2005**, *109*, 12663–12676.

24 Bratlie, K. M.; Lee, H.; Komvopoulos, K.; Yang, P.; Somorjai, G. A. Platinum Nanoparticle Shape Effects on Benzene Hydrogenation Selectivity. *Nano Lett.* **2007**, *7*, 3097–3101.

25 Matsumoto, F.; Roychowdhury, C.; DiSalvo, F. J.; Abruna, H. D. Electrocatalytic Activity of Ordered Intermetallic PtPb Nanoparticles Prepared by Borohydride Reduction toward Formic Acid Oxidation. *J. Electrochem. Soc.* **2008**, *155*, B148–B154.

26 Vitos, L.; Ruban, A. V.; Skriver, H. L.; Kollár, J. The Surface Energy of Metals. *Surf. Sci.* **1998**, *411*, 186–202.

27 Wang, Z. L. Transmission Electron Microscopy of Shape-Controlled Nanocrystals and Their Assemblies. *J. Phys. Chem. B* **2000**, *104*, 1153–1175.

28 Tian, N.; Zhou, Z.-Y.; Sun, S.-G.; Ding, Y.; Wang, Z. L. Synthesis of Tetrahexahedral Platinum Nanocrystals with High-Index Facets and High Electro-Oxidation Activity. *Science* **2007**, *316*, 732–735.

29 Yang, J.; Hu, W.; Chen, S.; Tang, J. Surface Self-Diffusion Behavior of a Pt Adatom on Wulff Polyhedral Clusters. *J. Phys. Chem. C* **2009**, *113*, 21501–21505.

30 Baletto, F.; Ferrando, R. Structural properties of nanoclusters: Energetic, thermodynamic, and kinetic effects. *Rev. Mod. Phys.* **2005**, *77*, 371–423.

31 Baletto, F.; Ferrando, R.; Fortunelli, A.; Montalenti, F.; Mottet, C. Crossover among Structural Motifs in Transition and Noble-Metal Clusters. *J. Chem. Phys.* **2002**, *116*, 3856–3863.

32 LaMer, V. K.; Dinegar, R. H. Theory, Production and Mechanism of Formation of Monodispersed Hydrosols. *J. Am. Chem. Soc.* **1950**, *72*, 4847–4854.

33 Biacchi, A. J.; Schaak, R. E. The Solvent Matters: Kinetic versus Thermodynamic Shape Control in the Polyol Synthesis of Rhodium Nanoparticles. *ACS Nano* **2011**, *5*, 8089–8099.

34 Chen, J.; Herricks, T.; Geissler, M.; Xia, Y. Single-Crystal Nanowires of Platinum Can Be Synthesized by Controlling the Reaction Rate of a Polyol Process. *J. Am. Chem. Soc.* **2004**, *126*, 10854–10855.

35 Song, H.; Kim, F.; Connor, S.; Somorjai, G. A.; Yang, P. Pt Nanocrystals: Shape Control and Langmuir−Blodgett Monolayer Formation. *J. Phys. Chem. B* **2004**, *109*, 188–193.

36 Zhang, J.; Fang, J. A General Strategy for Preparation of Pt 3d-Transition Metal (Co, Fe, Ni) Nanocubes. *J. Am. Chem. Soc.* **2009**, *131*, 18543–18547.

37 Zhang, J.; Yang, H.; Fang, J.; Zou, S. Synthesis and Oxygen Reduction Activity of Shape-Controlled Pt_3Ni Nanopolyhedra. *Nano Lett.* **2010**, *10*, 638–644.

38 Zhang, J.; Yang, H.; Yang, K.; Fang, J.; Zou, S.; Luo, Z.; Wang, H.; Bae, I.-T.; Jung, D. Y. Monodisperse Pt_3Fe Nanocubes: Synthesis, Characterization, Self-Assembly, and Electrocatalytic Activity. *Adv. Funct. Mater.* **2010**, *20*, 3727–3733.

39 Yang, H.; Zhang, J.; Sun, K.; Zou, S.; Fang, J. Enhancing by Weakening: Electrooxidation of Methanol on Pt_3Co and Pt Nanocubes. *Angew. Chem., Int. Ed.* **2010**, *49*, 6848–6851.

40 Loukrakpam, R.; Chang, P.; Luo, J.; Fang, B.; Mott, D.; Bae, I.-T.; Naslund, H. R.; Engelhard, M. H.; Zhong, C.-J. Chromium-Assisted Synthesis of Platinum Nanocube Electrocatalysts. *Chem. Commun. (Cambridge, U. K.)* **2010**, *46*, 7184–7186.

41 Xiao, Q.; Cai, M.; Balogh, M.; Tessema, M.; Lu, Y. Symmetric Growth of Pt Ultrathin Nanowires from Dumbbell Nuclei for Use as Oxygen Reduction Catalysts. *Nano Res.* **2012**, *5*, 145–151.

42 Sun, S.; Murray, C. B.; Weller, D.; Folks, L.; Moser, A. Monodisperse FePt Nanoparticles and Ferromagnetic FePt Nanocrystal Superlattices. *Science* **2000**, *287*, 1989–1992.

43 Chen, M.; Kim, J.; Liu, J. P.; Fan, H.; Sun, S. Synthesis of FePt Nanocubes and Their Oriented Self-Assembly. *J. Am. Chem. Soc.* **2006**, *128*, 7132–7133.

44 Kang, Y.; Murray, C. B. Synthesis and Electrocatalytic Properties of Cubic Mn−Pt Nanocrystals (Nanocubes). *J. Am. Chem. Soc.* **2010**, *132*, 7568–7569.

45 Liu, Y.; Li, D.; Stamenkovic, V. R.; Soled, S.; Henao, J. D.; Sun, S. Synthesis of Pt_3Sn Alloy Nanoparticles and Their Catalysis for Electro-Oxidation of CO and Methanol. *ACS Catal.* **2011**, *1*, 1719–1723.

46 Choi, S.-I.; Choi, R.; Han, S. W.; Park, J. T. Shape-Controlled Synthesis of Pt_3Co Nanocrystals with High Electrocatalytic Activity toward Oxygen Reduction. *Chem.—Eur. J.* **2011**, *17*, 12280–12284.

47 Kang, Y.; Pyo, J. B.; Ye, X.; Gordon, T. R.; Murray, C. B. Synthesis, Shape Control, and Methanol Electro-oxidation Properties of Pt−Zn Alloy and Pt_3Zn Intermetallic Nanocrystals. *ACS Nano* **2012**, *6*, 5642–5647.

48 Kang, Y.; Qi, L.; Li, M.; Diaz, R. E.; Su, D.; Adzic, R. R.; Stach, E.; Li, J.; Murray, C. B. Highly active Pt_3Pb and core-shell Pt_3Pb-Pt electrocatalysts for formic acid oxidation. *ACS Nano* **2012**, *6*, 2818–2825.

49 Kang, Y.; Ye, X.; Murray, C. B. Size- and Shape-Selective Synthesis of Metal Nanocrystals and Nanowires Using CO as a Reducing Agent. *Angew. Chem., Int. Ed.* **2010**, *49*, 6156–6159.

50 Wu, B.; Zheng, N.; Fu, G. Small molecules control the formation of Pt nanocrystals: a key role of carbon monoxide in the synthesis of Pt nanocubes. *Chem. Commun. (Cambridge, U. K.)* **2011**, *47*, 1039–1041.

51 Wu, J.; Gross, A.; Yang, H. Shape and Composition-Controlled Platinum Alloy Nanocrystals Using Carbon Monoxide as Reducing Agent. *Nano Lett.* **2011**, *11*, 798–802.

52 Wu, J.; Qi, L.; You, H.; Gross, A.; Li, J.; Yang, H. Icosahedral Platinum Alloy Nanocrystals with Enhanced Electrocatalytic Activities. *J. Am. Chem. Soc.* **2012**, *134*, 11880–11883.

53 Xiong, Y.; Cai, H.; Wiley, B. J.; Wang, J.; Kim, M. J.; Xia, Y. Synthesis and Mechanistic Study of Palladium Nanobars and Nanorods. *J. Am. Chem. Soc.* **2007**, *129*, 3665–3675.

54 Yu, D.; Yam, V. W.-W. Controlled Synthesis of Monodisperse Silver Nanocubes in Water. *J. Am. Chem. Soc.* **2004**, *126*, 13200–13201.

55 Yin, A.-X.; Min, X.-Q.; Zhang, Y.-W.; Yan, C.-H. Shape-Selective Synthesis and Facet-Dependent Enhanced Electrocatalytic Activity and Durability of Monodisperse Sub-10 nm Pt–Pd Tetrahedrons and Cubes. *J. Am. Chem. Soc.* **2011**, *133*, 3816–3819.

56 Quan, Z.; Wang, Y.; Fang, J. High-Index Faceted Noble Metal Nanocrystals. *Acc. Chem. Res.* **2013**, *46*, 191–202.

57 Wei, L.; Fan, Y.-J.; Tian, N.; Zhou, Z.-Y.; Zhao, X.-Q.; Mao, B.-W.; Sun, S.-G. Electrochemically Shape-Controlled Synthesis in Deep Eutectic Solvents—A New Route to Prepare Pt Nanocrystals Enclosed by High-Index Facets with High Catalytic Activity. *J. Phys. Chem. C* **2012**, *116*, 2040–2044.

58 Yu, T.; Kim, D. Y.; Zhang, H.; Xia, Y. Platinum Concave Nanocubes with High-Index Facets and Their Enhanced Activity for Oxygen Reduction Reaction. *Angew. Chem., Int. Ed.* **2011**, *50*, 2773–2777.

59 Zhang, H.; Jin, M.; Wang, J.; Li, W.; Camargo, P. H. C.; Kim, M. J.; Yang, D.; Xie, Z.; Xia, Y. Synthesis of Pd–Pt Bimetallic Nanocrystals with a Concave Structure through a Bromide-Induced Galvanic Replacement Reaction. *J. Am. Chem. Soc.* **2011**, *133*, 6078–6089.

60 Yin, A.-X.; Min, X.-Q.; Zhu, W.; Liu, W.-C.; Zhang, Y.-W.; Yan, C.-H. Pt-Cu and Pt-Pd-Cu Concave Nanocubes with High-Index Facets and Superior Electrocatalytic Activity. *Chem.—Eur. J.* **2012**, *18*, 777–782.

61 Qiu, H.; Zou, F. Nanoporous PtCo Surface Alloy Architecture with Enhanced Properties for Methanol Electrooxidation. *ACS Appl. Mater. Interfaces* **2012**, *4*, 1404–1410.

62 Wang, C.; Chi, M.; Wang, G.; van der Vliet, D.; Li, D.; More, K.; Wang, H.-H.; Schlueter, J. A.; Markovic, N. M.; Stamenkovic, V. R. Correlation Between Surface Chemistry and Electrocatalytic Properties of Monodisperse Pt_xNi_{1-x} Nanoparticles. *Adv. Funct. Mater.* **2011**, *21*, 147–152.

63 Roth, C.; Papworth, A. J.; Hussain, I.; Nichols, R. J.; Schiffrin, D. J. A Pt/Ru Nanoparticulate System to Study the Bifunctional Mechanism of Electrocatalysis. *J. Electroanal. Chem.* **2005**, *581*, 79–85.

64 Liu, Y.; Chi, M.; Mazumder, V.; More, K. L.; Soled, S.; Henao, J. D.; Sun, S. Composition-Controlled Synthesis of Bimetallic PdPt Nanoparticles and Their Electro-oxidation of Methanol. *Chem. Mater.* **2011**, *23*, 4199–4203.

65 Toda, T.; Igarashi, H.; Uchida, H.; Watanabe, M. Enhancement of the Electroreduction of Oxygen on Pt Alloys with Fe, Ni, and Co. *J. Electrochem. Soc.* **1999**, *146*, 3750–3756.

66 Wu, J.; Zhang, J.; Peng, Z.; Yang, S.; Wagner, F. T.; Yang, H. Truncated Octahedral Pt3Ni Oxygen Reduction Reaction Electrocatalysts. *J. Am. Chem. Soc.* **2010**, *132*, 4984–4985.

67 Grgur, B. N.; Marković, N. M.; Ross, P. N. Underpotential Deposition of Lead on Pt(111) in Perchloric Acid Solution: RRDPt(111)E Measurements. *Langmuir* **1997**, *13*, 6370–6374.

68 Gasteiger, H. A.; Ross, P. N. Oxygen Reduction on Platinum Low-Index Single-Crystal Surfaces in Alkaline Solution: Rotating Ring Disk Pt(hkl) Studies. *J. Phys. Chem.* **1996**, *100*, 6715–6721.

69 Marković, N. M.; Adžić, R. R.; Cahan, B. D.; Yeager, E. B. Structural Effects in Electrocatalysis: Oxygen Reduction on Platinum Low Index Single-Crystal Surfaces in Perchloric Acid Solutions. *J. Electroanal. Chem.* **1994**, *377*, 249–259.

70 Markovic, N. M.; Gasteiger, H. A.; Ross, P. N. Oxygen Reduction on Platinum Low-Index Single-Crystal Surfaces in Sulfuric Acid Solution: Rotating Ring-Pt(hkl) Disk Studies. *J. Phys. Chem.* **1995**, *99*, 3411–3415.

71 Niu, Z.; Wang, D.; Yu, R.; Peng, Q.; Li, Y. Highly branched Pt-Ni nanocrystals enclosed by stepped surface for methanol oxidation. *Chem. Sci.* **2012**, *3*, 1925–1929.

72 Lim, B.; Jiang, M.; Camargo, P. H. C.; Cho, E. C.; Tao, J.; Lu, X.; Zhu, Y.; Xia, Y. Pd-Pt Bimetallic Nanodendrites with High Activity for Oxygen Reduction. *Science* **2009**, *324*, 1302–1305.

73 Peng, Z.; Yang, H. Synthesis and Oxygen Reduction Electrocatalytic Property of Pt-on-Pd Bimetallic Heteronanostructures. *J. Am. Chem. Soc.* **2009**, *131*, 7542–7543.